Electronic Supplementary Information for

Photodriven Hydrogen Evolution by Molecular Catalysts Using Al_2O_3-Protected Perylene-3,4-dicarboximide on NiO Electrodes

Rebecca J. Kamire, Marek B. Majewski, William L. Hoffeditz, Brian T. Phelan, Omar K. Farha, Joseph T. Hupp, and Michael R. Wasielewski*

Department of Chemistry and Argonne-Northwestern Solar Energy Research (ANSER) Center, Northwestern University, Evanston, IL 60208-3113, USA

*Address correspondence to this author. E-mail: m-wasielewski@northwestern.edu

Contents:

I. Experimental details

Materials and synthesis

Materials and reagents were obtained from commercial sources and used without further purification. Toluene for dye loading was dried using a Glass Contour solvent system. Electrochemical quality acetonitrile for photoelectrochemical experiments was purchased from Sigma-Aldrich. The **PMI** dye and **PMI diester**,[1] cobaloxime catalyst,[2] and nickel catalyst[3] were prepared following literature procedures.

Film preparation

Films were prepared based on a literature procedure.[4] To 1.0 g $NiCl_2$ and 1.0 g triblock co-polymer (F108, Sigma-Aldrich) was added 3.0 g ultrapure H_2O and 6.0 g EtOH. This mixture was mixed and sonicated until most of the material was dissolved in a cloudy green emulsion, then allowed to sit for three days. It was then centrifuged at 3000 rpm for 10 min, after which the supernatant was used to prepare the films. Fluorine-doped tin oxide (FTO) coated glass plates (Hartford Glass, TEC 15) were first sonicated in an Alconox solution for 15 min, rinsed with water, sonicated in ethanol for 15 min, sonicated in methanol for 15 min, and then dried under a nitrogen stream. The $NiCl_2$ solution was applied using the doctor blade method to a 1 cm^2 rectangular active area for the fsTA measurements or a 0.38 cm^2 circular active area for the electrochemical experiments. The films were dried in an oven at 110 °C for 15 min then placed in a furnace at 450 °C for 30 min. More $NiCl_2$ solution was applied and annealed two more times for a total of three cycles. The thicknesses of the nanostructured NiO films were measured as about 0.8 or 1.0 μm for circles (electrochemical experiments) or rectangles (fsTA experiments), respectively, using a Veeco Dektak 150 stylus profiler. Films were stored in a 110 °C oven until dye loading.

Films were soaked with gentle shaking in a 0.45 mM solution of **PMI** in 1:3 toluene:methanol in the dark overnight, then rinsed with CH_2Cl_2 and dried under a nitrogen stream. Atomic layer deposition (ALD) of Al_2O_3 was performed in a Savannah 100 reactor manufactured by Ultratech/Cambridge Nano-Tech. using dimethylaluminum isopropoxide, purchased from Strem Chemicals, at 80 °C as the precursor. The deposition chamber was held at 110 °C, and alternating exposure cycles of Al (0.05 s pulse, 10 s exposure, 30 s nitrogen purge) and water (0.02 s pulse, 10 s exposure, 30 s nitrogen purge) were applied. The typical growth rate is about 1 Å per cycle measured on a J.A. Woollam Co. M-2000U ellipsometer.

UV-vis spectroscopy standards were prepared by spin-coating samples of **PMI diester** onto 2.5 × 2.5 cm glass microscope slides. A **PMI diester**:CH_2Cl_2 mixture was prepared in a 1:100 ratio by mass, and 0.04 mL was spin coated onto at 1,000 rpm for 10 s. A **PMI diester**:poly(methyl methacrylate) (Aldrich, 12,000):CH_2Cl_2 mixture was prepared in a 1:60:600 ratio by mass, and 0.04 mL was spin coated onto a separate slide at 2,000 rpm for 15 s.

Computational methods

The ground state singlet geometry of **PMI diester** was initially relaxed via molecular mechanics with the MMFF94s force field through implementation of the Avogadro 1.1.0 software.[5] The geometries were further relaxed using density functional theory (DFT) as implemented in TeraChem 1.5 K software.[6] All DFT calculations were performed using the B3LYP exchange-correlation functional[7-10] with a split-valence double zeta basis set with added polarization functions (6-31G*). Visualizations of the optimized structures were generated using PyMol 1.2r1.[11]

Optical spectroscopy

UV-Vis transmission spectra of the films were acquired using a Perkin Elmer LAMBDA 1050 spectrophotometer equipped with a 150 mm integrating sphere. The FTO │NiO background was subtracted to yield the reported spectra.

Femtosecond transient absorption spectroscopy (fsTA) experiments were conducted using a regeneratively amplified Ti:sapphire laser system with samples translated in two dimensions and irradiated at 495 nm as previously described.[1, 12] All fsTA data were corrected for group delay dispersion (GDD, or "chirp") and t_0 prior to kinetic analysis. Single wavelength kinetic analysis was performed using a nonlinear least-squares fit to a sum of exponentials convoluted with a Gaussian instrument response function, which fit to about 0.3 ps. The three-dimensional fsTA data sets were analyzed by singular value decomposition (SVD) and global fitting to obtain the kinetic time constants and species-associated spectra (SAS) in MATLAB[13] using home-written programs as previously described.[1] The Al_2O_3 │ **PMI** data set was fit to an A → B → C → ground state (GS) model, where the initial population of A was fixed as 100%. The NiO │ **PMI** │ (ALD, catalyst) data sets were fit to an A → B → C → D → GS model, where the initial populations of A:B were set to 1:1 to account for the **PMI** population that injects holes into NiO within the instrument response time.

Electrochemistry and photoelectrochemistry

Electrochemical measurements were performed using a CH Instruments Model 660A or 750E electrochemical workstation. All measurements were performed under argon using either a 3.0 mm diameter glassy carbon electrode or a dye-functionalized film as the working electrode, a 3.0 mm diameter glassy carbon counter electrode, and an Ag/AgCl (3 M NaCl) reference electrode. Light was applied from two LEDs (CREE XP-G2 neutral white, RapidLED, 100 mW/cm^2 incident

on the sample per LED) covered with 410 nm long-pass filters. Because there is some NiO batch-to-batch variability, all of these films for each set of experiments were fabricated together and each experiment was performed on two identical films. The LEDs were oriented on an aluminum sheet heat sink in an orientation that allowed the sample cell to be illuminated from the front and rear, with respect to the working surface of the electrode. Light pulse timing of the LEDs was controlled by a 12V relay cycle timer module programmed for 10s intervals. Linear sweep voltammetry experiments were performed at 5 mV/s.

Photoelectrochemical H_2 generation

Photocatalysis experiments were performed under the same conditions as the electrochemistry experiments but in a sealed cell under argon with 2.5 mL of solution and 20.2 mL of headspace. A -0.40 V bias was applied concurrent with illumination for two hours. The H_2 in the headspace was identified following triplicate injections of 300 μL each into a gas chromatograph (Shimadzu GC-2014) equipped with a 5 Å molsieve column, Ar carrier gas, and a thermal conductivity detector. It was quantified with respect to a calibration curve produced from injections of standard amounts of hydrogen into the gas chromatograph. Faradaic efficiencies were calculated from the amount of H_2 in the headspace and the amount of current passed during the experiment. The values reported are averages with standard deviations of measurements on 2-3 films.

II. UV-Vis absorption spectra

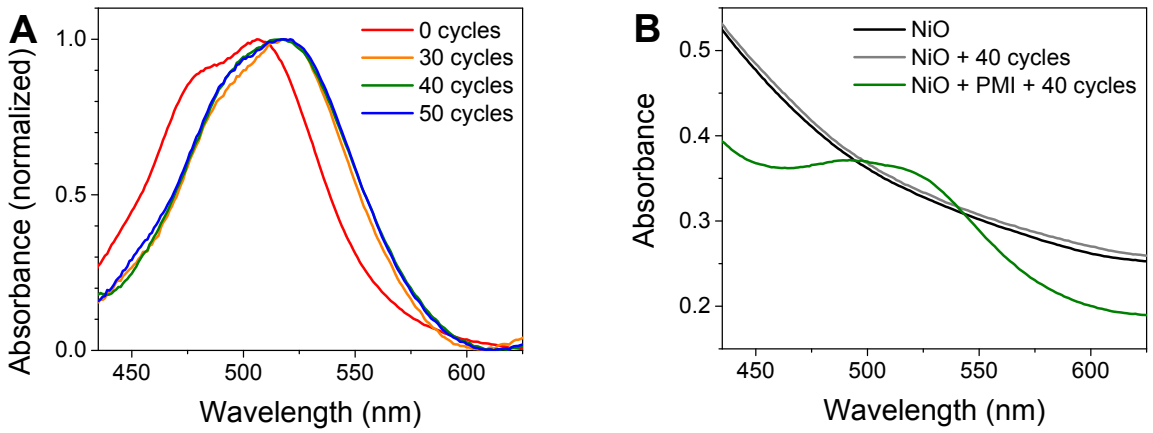

Figure S1. (A) Normalized UV-Vis absorption spectra of NiO | **PMI** films treated with 0, 30, 40, and 50 cycles of Al_2O_3 ALD. The NiO background is subtracted. (B) UV-Vis absorption spectra of films treated without and with 40 cycles of Al_2O_3 ALD before background subtraction or normalization.

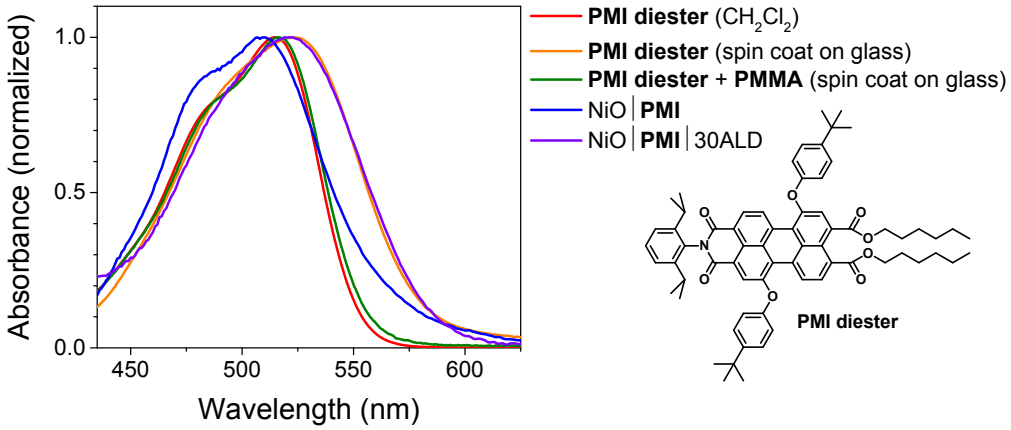

Figure S2. Normalized UV-Vis absorption spectra of **PMI diester** in CH_2Cl_2 (red), **PMI diester** spin coated on glass (orange) or on glass with PMMA (green), NiO | **PMI** (blue), and NiO | **PMI** | 30 cycles of Al_2O_3 ALD (purple). The solvent and substrate backgrounds are subtracted. **PMI diester** was synthesized as previously reported, where the molecule was found to be a good model for **PMI** bound to a semiconductor surface.[1] The absorption spectra for **PMI diester** were collected using a Shimadzu 1800 Spectrometer.

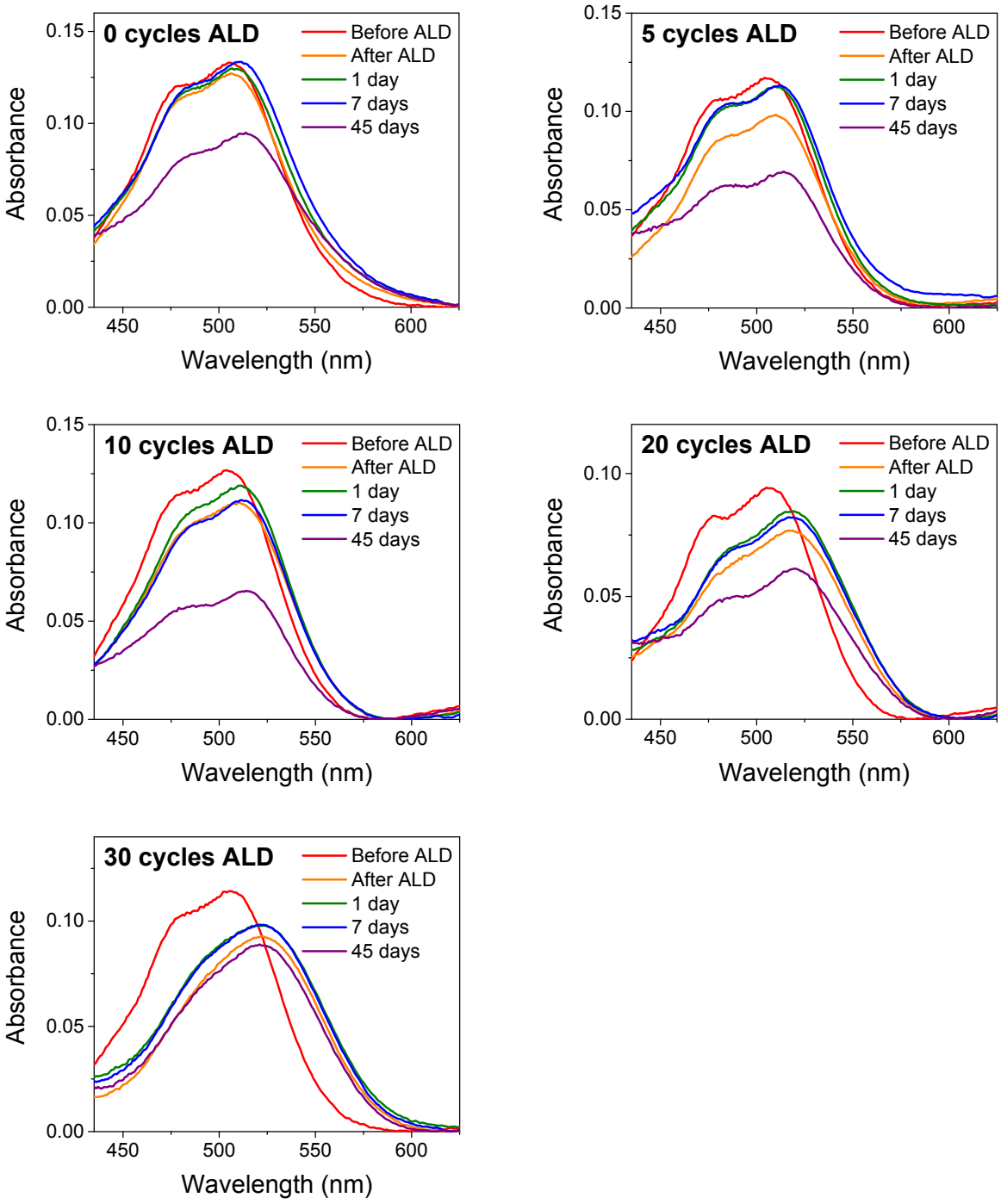

Figure S3. UV-Vis absorption spectra of NiO | **PMI** | ALD films before and after 0-30 cycles of ALD of Al_2O_3 and 0-45 days of aging in air and ambient light. The "After ALD" spectra were collected about 8 h after the "Before ALD" spectra. The NiO | **PMI** | 0ALD film was stored in the dark under air while ALD was performed on the other films. The NiO background is subtracted.

III. Electrochemistry

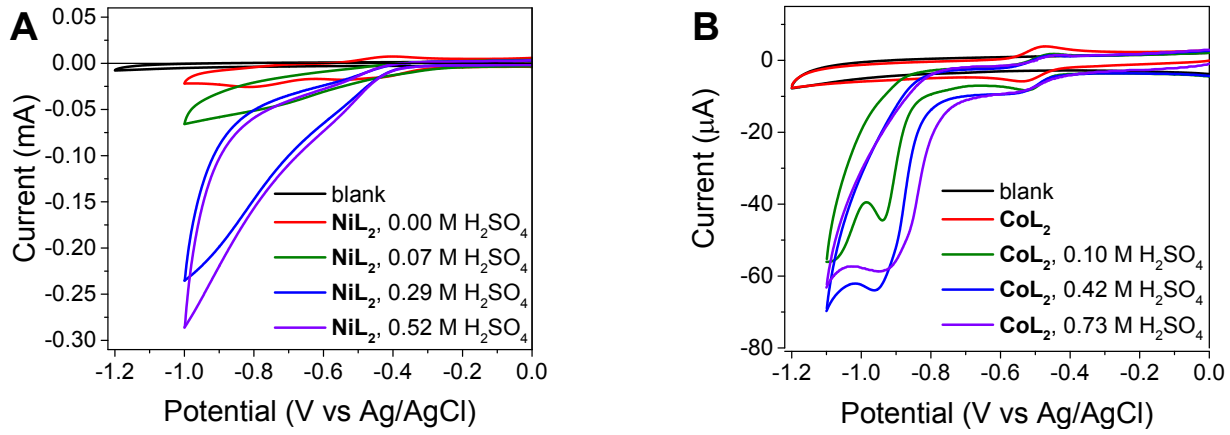

Figure S4. Cyclic voltammograms of (A) 0.5 mM **NiL_2** and (B) 0.5 mM **CoL_2** with increasing acid concentration. (Conditions: 1.0 mM Fc and 0.1 M Na_2SO_4 in 1:1 H_2O:MeCN; under argon; 100 mV/s; Working = GC; Ref = Ag/AgCl; Counter = GC)

IV. Femtosecond transient absorption spectroscopy

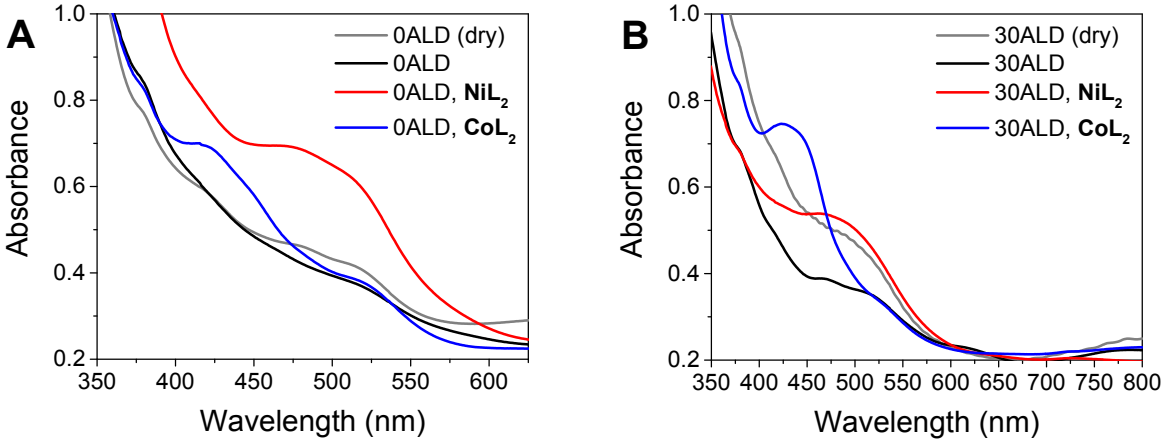

Figure S5. UV-Vis absorption spectra of (A) NiO **|** **PMI** and (B) NiO **|** **PMI** **|** 30ALD dry films under nitrogen ("dry") and in 0.1 M H_2SO_4/0.1 M Na_2SO_4 in 1:1 MeCN:H_2O with and without 0.5 mM **NiL_2** or **CoL_2** under argon for study by fsTA spectroscopy. The spectra were collected using a Shimadzu 1800 Spectrometer, and the NiO background was not subtracted.

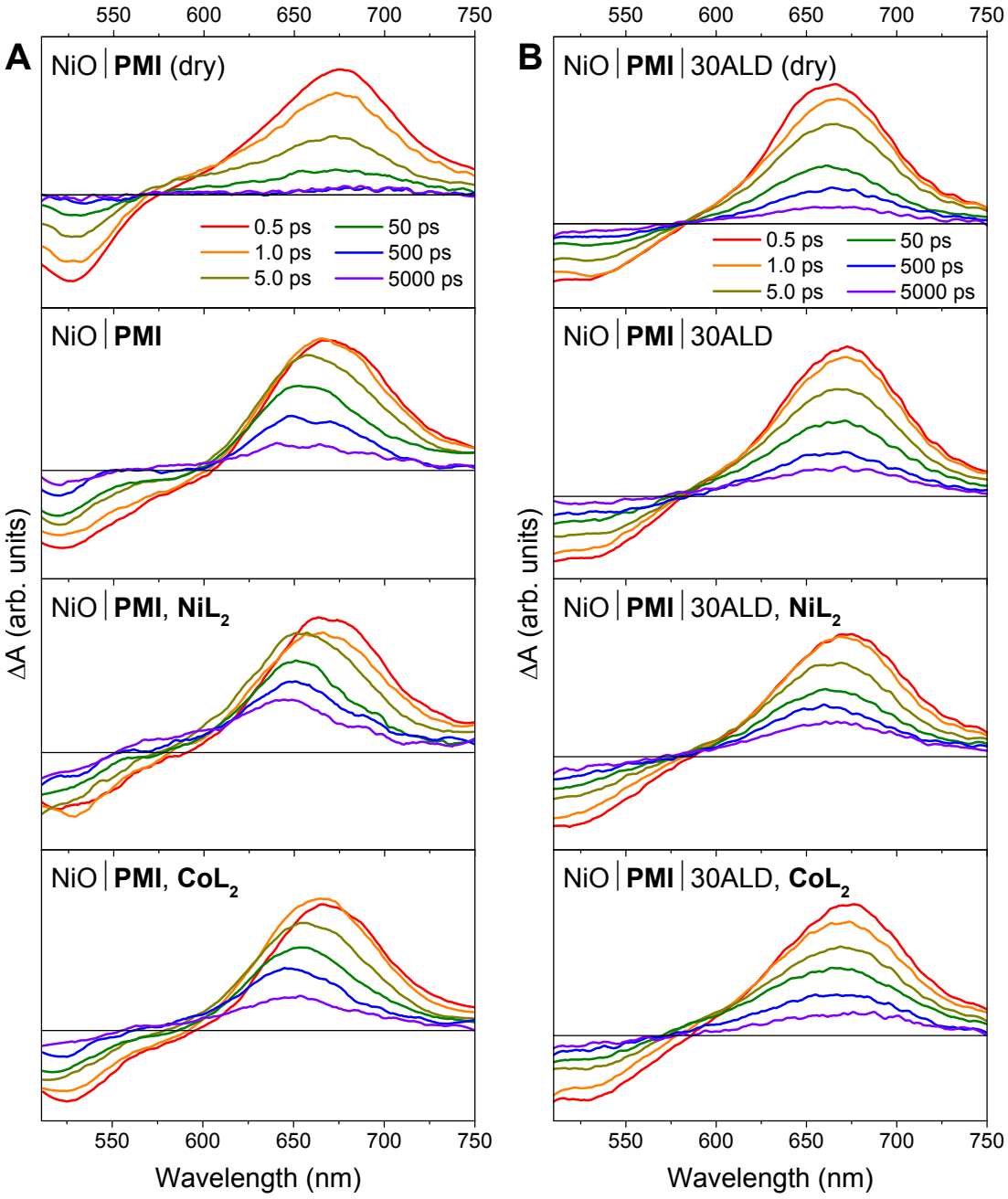

Figure S6. fsTA spectra of (A) NiO | **PMI** and (B) NiO | **PMI** | 30ALD films dry under nitrogen ("dry") and in 0.1 M H_2SO_4/0.1 M Na_2SO_4 in 1:1 MeCN:H_2O with and without 0.5 mM **NiL_2** or **CoL_2** under argon following excitation with a 495 nm laser pulse.

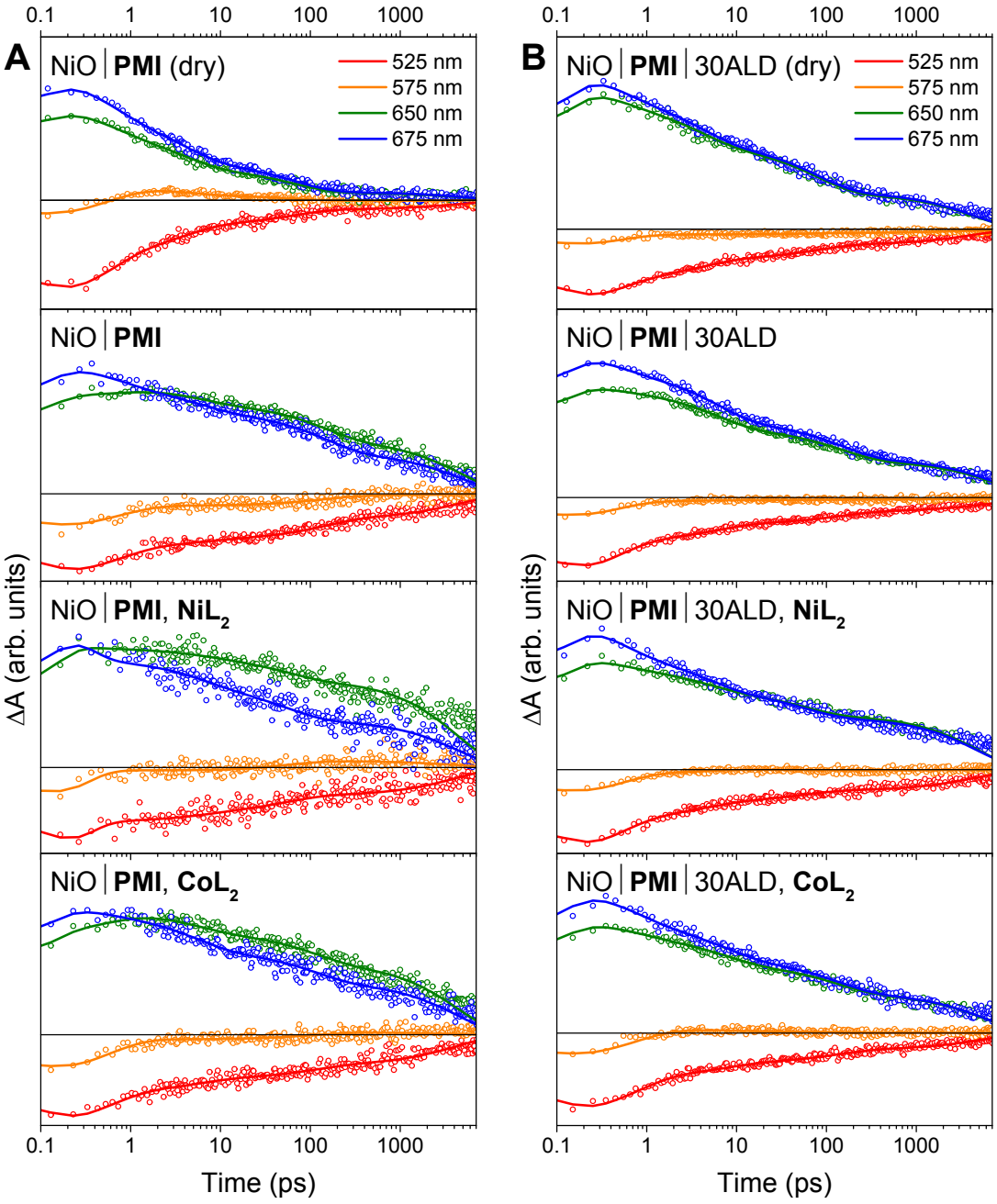

Figure S8. Kinetic results of SVD and global fitting of the fsTA data (Figure S6) at selected wavelengths to an A → B → C → D → GS model.

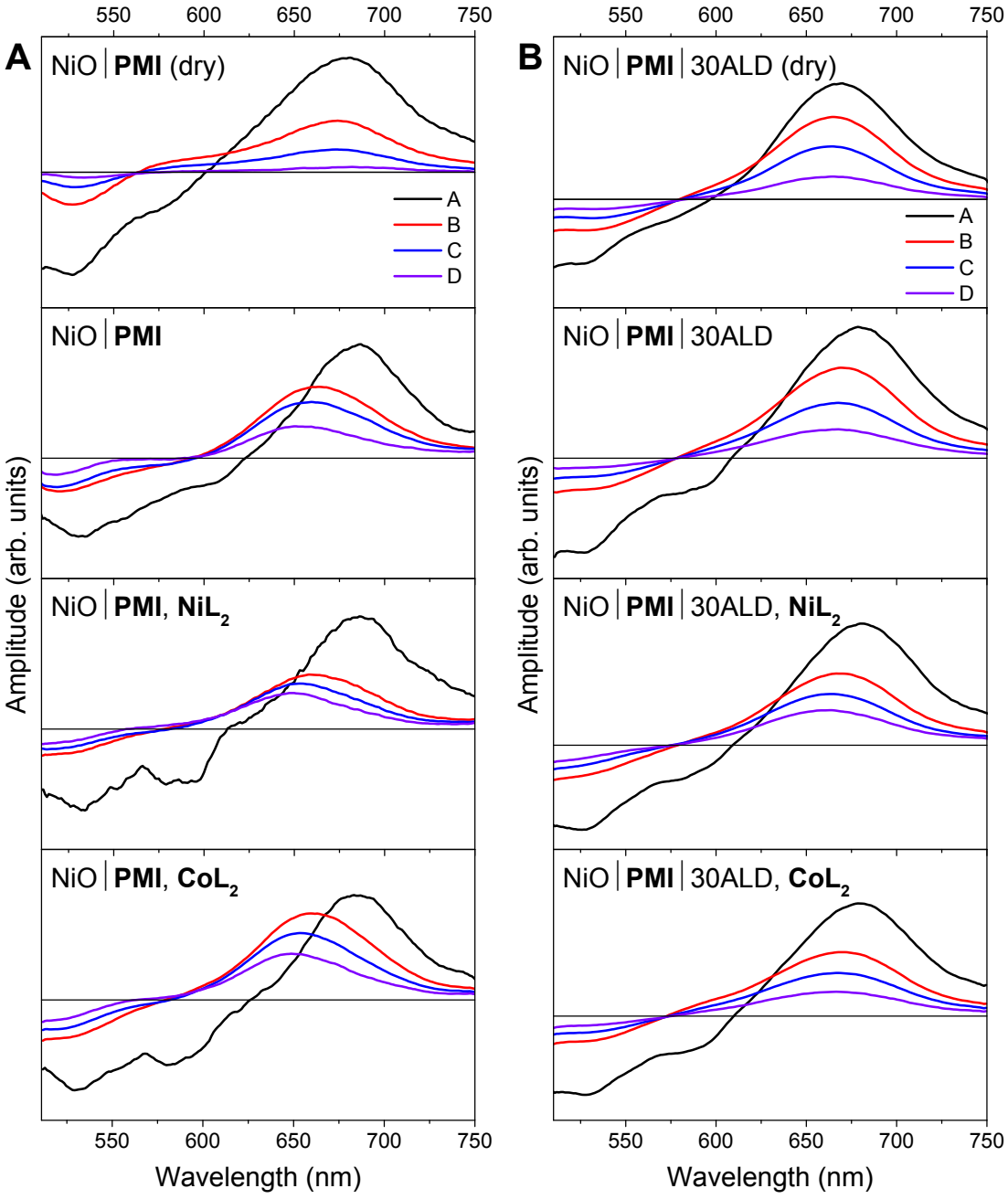

Figure S9. Species-associated spectra resulting from SVD and global fitting (Figure S8) of the fsTA data (Figures S6) at selected wavelengths to an A → B → C → D → GS model.

Table S1. fsTA fits of Semiconductor | **PMI** | (ALD) + (catalyst) to A → B → C → D → GS models

	τ_{CS} [b] A → B (ps)	τ_{CR1} [c] B → C (ps)	τ_{CR2} [c] C → D (ps)	τ_{CR3} [c] D → GS (ns)
Al_2O_3 | **PMI** (dry)[a]	-	4.2 ± 0.3	320 ± 20	13.6 ± 0.7
NiO | **PMI** (dry)	0.6 ± 0.3	3.9 ± 0.3	66 ± 3	5.2 ± 0.1
NiO | **PMI** | 30ALD (dry)	0.5 ± 0.3	4.0 ± 0.3	77 ± 3	4.34 ± 0.09
NiO | **PMI**	0.8 ± 0.3	6 ± 1	147 ± 8	4.93 ± 0.03
NiO | **PMI**, **NiL_2**	0.2 ± 0.3	6 ± 2	55 ± 9	4.33 ± 0.03
NiO | **PMI**, **CoL_2**	0.6 ± 0.3	5.5 ± 0.8	110 ± 10	4.35 ± 0.05
NiO | **PMI** | 30ALD	0.4 ± 0.3	5.9 ± 0.3	144 ± 5	8.10 ± 0.03
NiO | **PMI** | 30ALD, **NiL_2**	0.5 ± 0.3	4.5 ± 0.7	55 ± 5	4.80 ± 0.03
NiO | **PMI** | 30ALD, **CoL_2**	0.7 ± 0.3	7.5 ± 0.7	133 ± 8	5.8 ± 0.1

[a] Data first reported in Ref. 28; now, the decay of ^{1}***PMI** was fit to an A → B → C → GS model. [b] Charge separation begins during the instrument response time. [c] If catalyst reduction occurs, it most likely occurs during the charge recombination timescales.

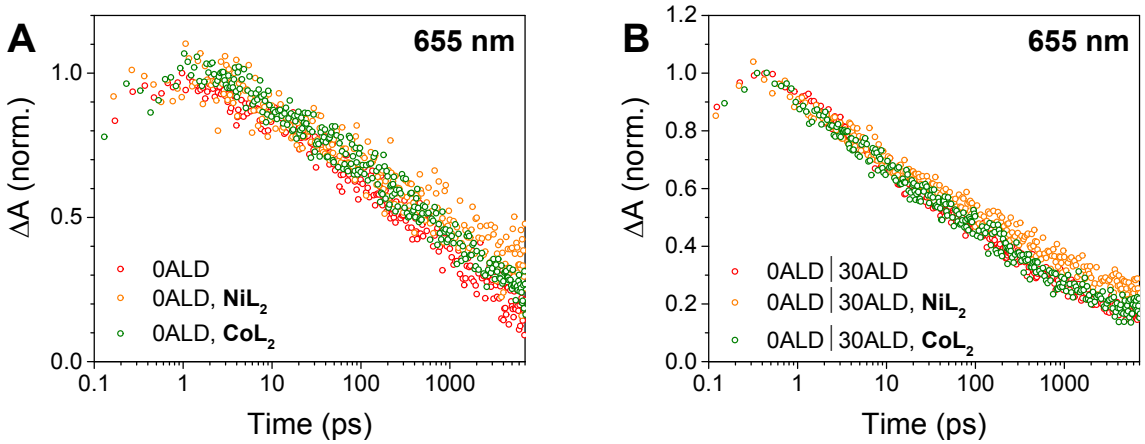

Figure S10. Single wavelength traces from the fsTA data (Figure S6) at 655 nm.

V. Photoelectrochemical experiments

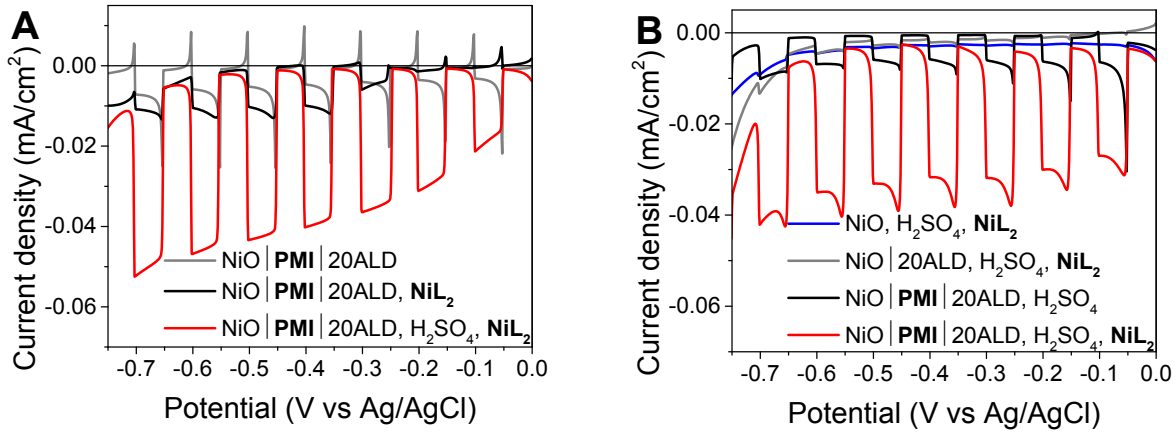

Figure S11. Linear sweep voltammetry measurements on NiO | (**PMI**) | (20 cycles Al_2O_3 ALD) working electrodes with 10 s light on/off cycles (A) starting without 0.1 M H_2SO_4 (scans made in order on the same film with sequential NiL_2 and H_2SO_4 additions) and (B) starting with 0.1 M H_2SO_4 (red follows black on the same film). Catalyst was added to make 0.5 mM **NiL_2**. The red curves in (A) and (B) are different because of the previous deleterious effect on the film in (B) of scanning to very negative potentials in the presence of acid without catalyst (black). (Conditions: 0.1 M Na_2SO_4 and 1 mM ferrocene in 1:1 H_2O:MeCN; under argon; 200 mW/cm^2 white light with 410 nm long-pass filters; Ref = Ag/AgCl; Counter = GC; rate 5 mV/s from 0.00 V to -0.75 V)

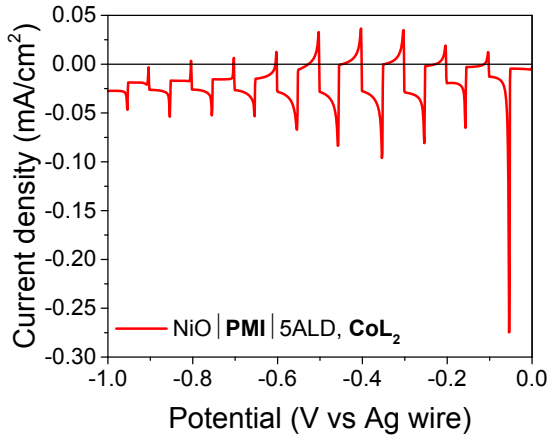

Figure S12. Linear sweep voltammetry measurements on NiO | (**PMI**) | (5 cycles Al_2O_3 ALD) working electrodes with 10 s light on/off cycles with 0.4 mM **CoL_2**. (Conditions: 0.05 M KPi (pH 7) in 2:1 H_2O:MeCN; under argon; 200 mW/cm^2 white light; Pseudoreference = Ag wire; Counter = Pt mesh; rate 5 mV/s from 0.00 V to -0.55 V)

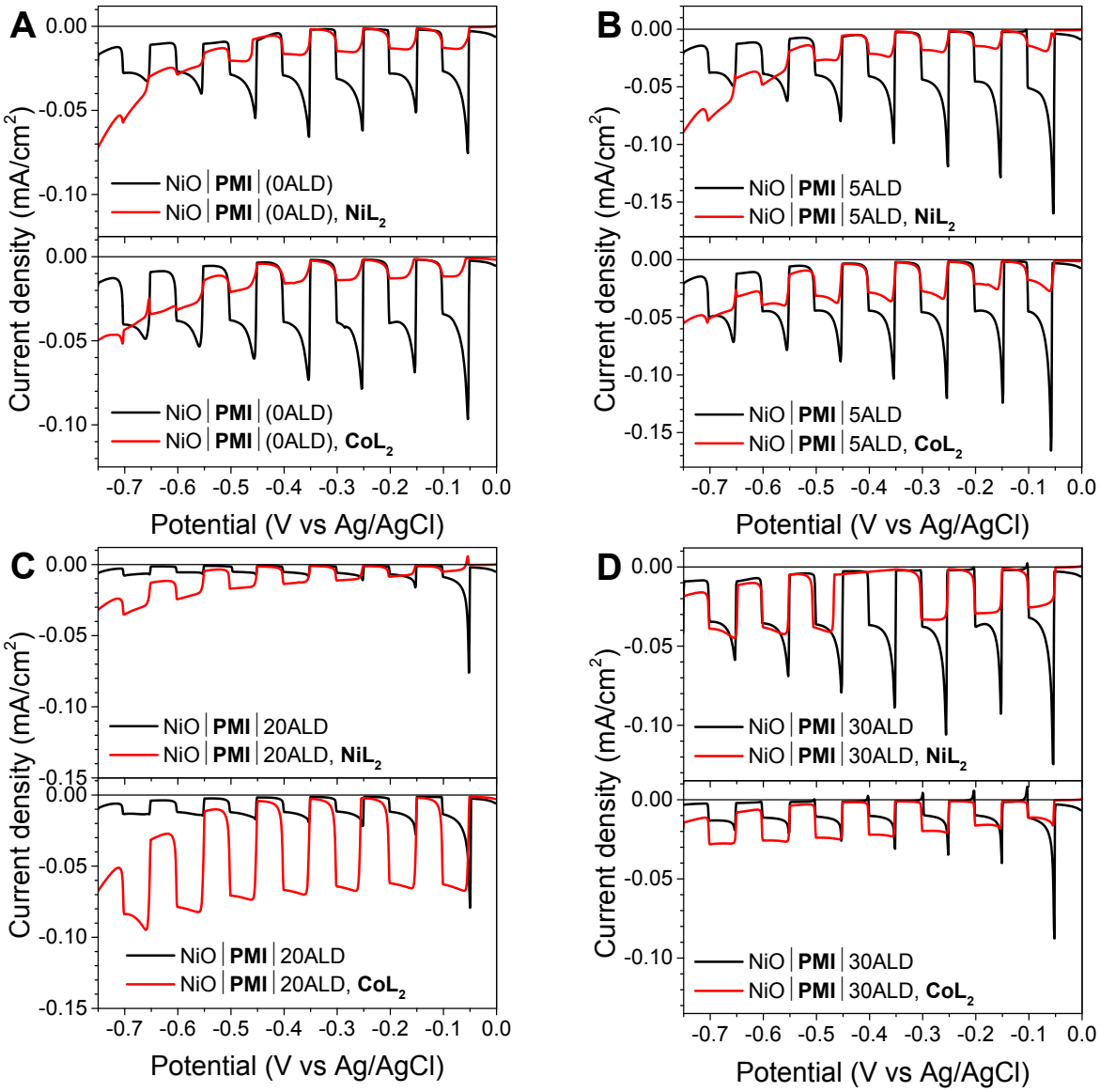

Figure S13. Linear sweep voltammetry measurements on NiO | **PMI** | ALD working electrodes with (A) 0, (B) 5, (C) 20, and (D) 30 cycles of Al_2O_3 ALD with 10 s light on/off cycles. Measurements were first made on NiO | **PMI** | ALD films (black) followed by addition of 0.5 mM $\mathbf{NiL_2}$ or 0.5 mM $\mathbf{CoL_2}$ (red). (Conditions: 0.1 M H_2SO_4 and 0.1 M Na_2SO_4 in 1:1 H_2O:MeCN; 200 mW/cm^2 white light with 410 nm long-pass filters; under argon; Ref = Ag/AgCl; Counter = GC; scan 5 mV/s from 0.00 V to -0.80 V)

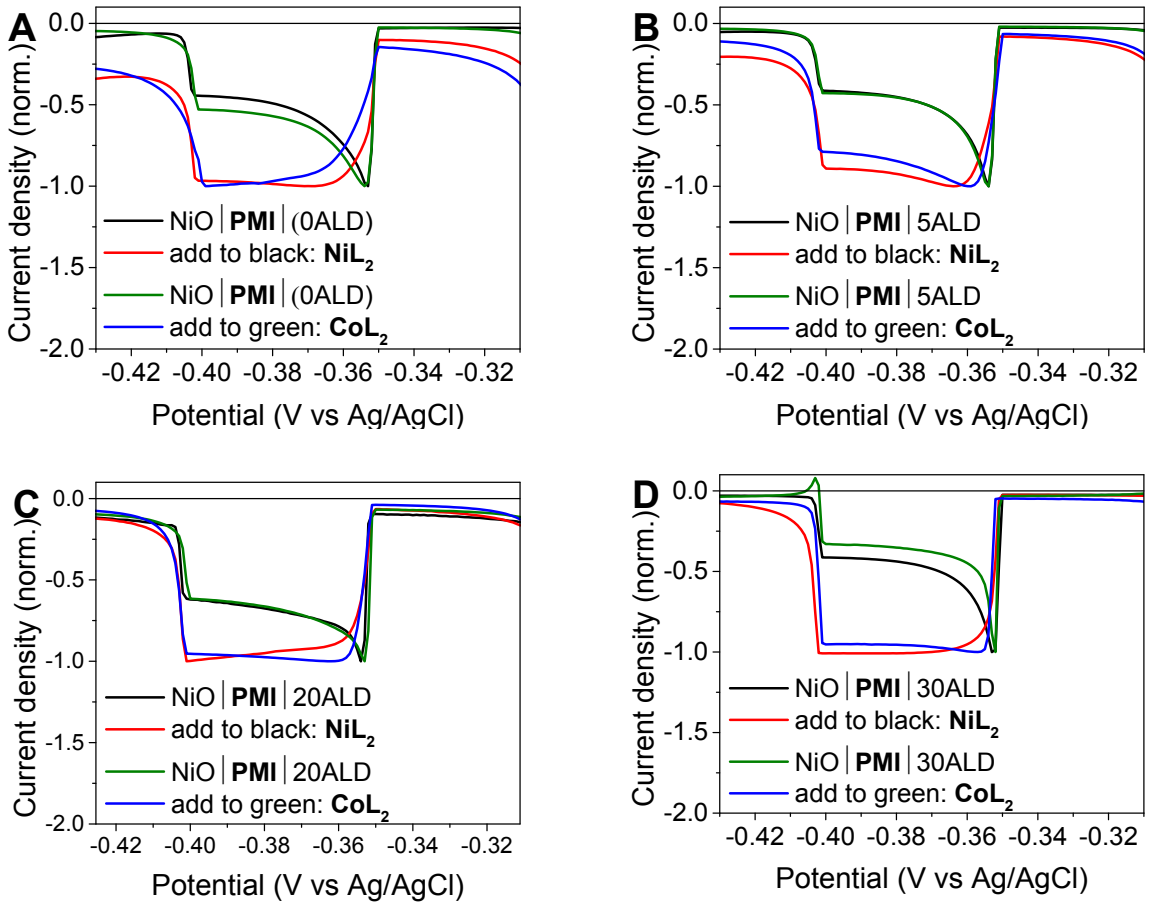

Figure S14. Normalized linear sweep voltammetry measurements from Figure S13 on NiO | **PMI** | ALD working electrodes with 0-30 cycles of Al_2O_3 ALD. Measurements were first made on NiO | **PMI** | ALD films (black, green) followed by addition of 0.5 mM **NiL_2** or 0.5 mM **CoL_2** (red, blue), respectively. (Conditions: 0.1 M H_2SO_4 and 0.1 M Na_2SO_4 in 1:1 H_2O:MeCN; 200 mW/cm^2 white light with 410 nm long-pass filters; under argon; Ref = Ag/AgCl; Counter = GC; scan 5 mV/s from 0.00 V to -0.80 V)

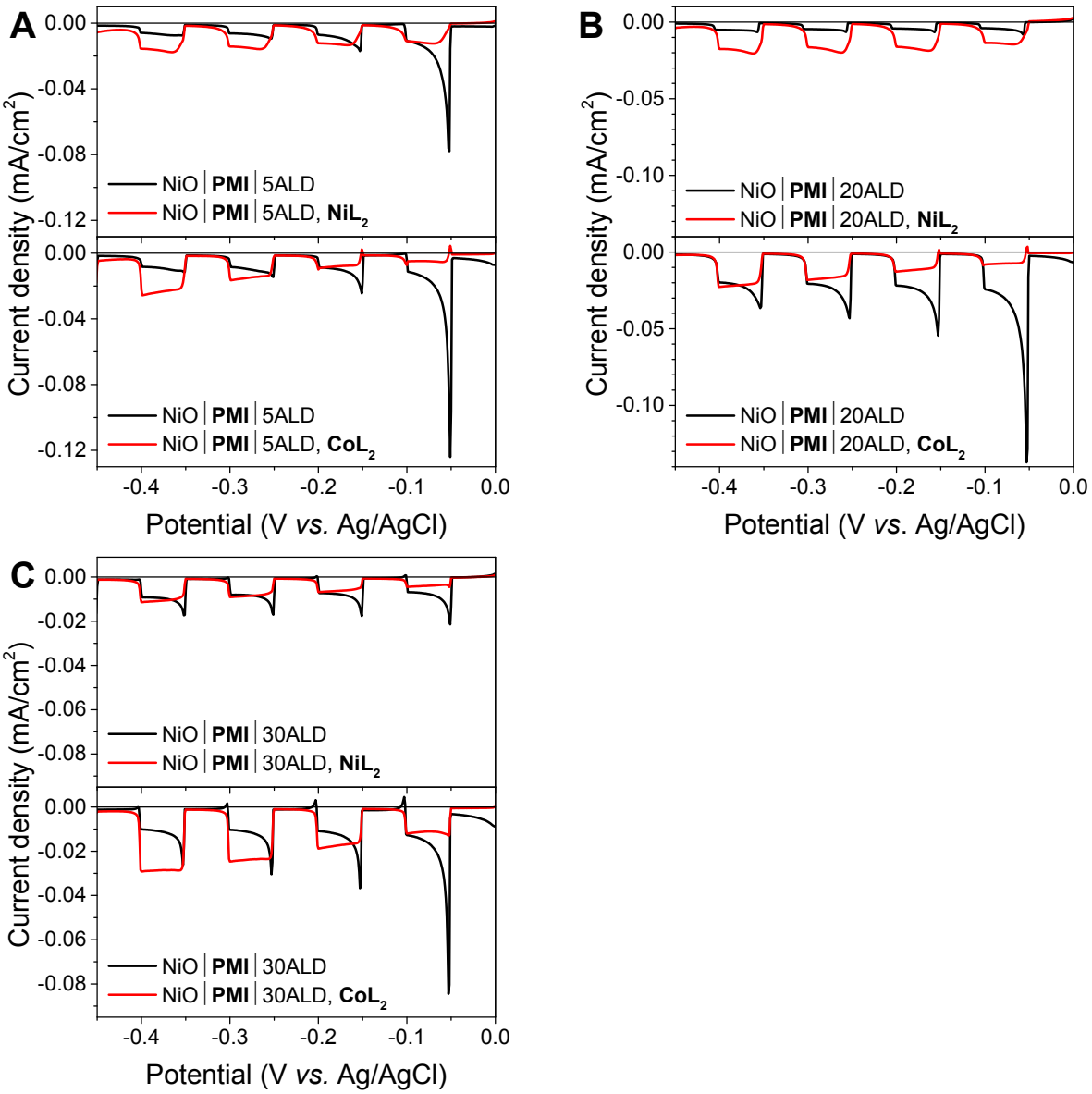

Figure S15. Duplicate linear sweep voltammetry experiments compared to Figure S13, except potentials were not scanned more negative than -0.45 V *vs*. Ag/AgCl. LSV measurements on NiO | **PMI** | ALD working electrodes with (A) 5, (B) 20, and (C) 30 cycles of Al_2O_3 ALD with 10 s light on/off cycles.

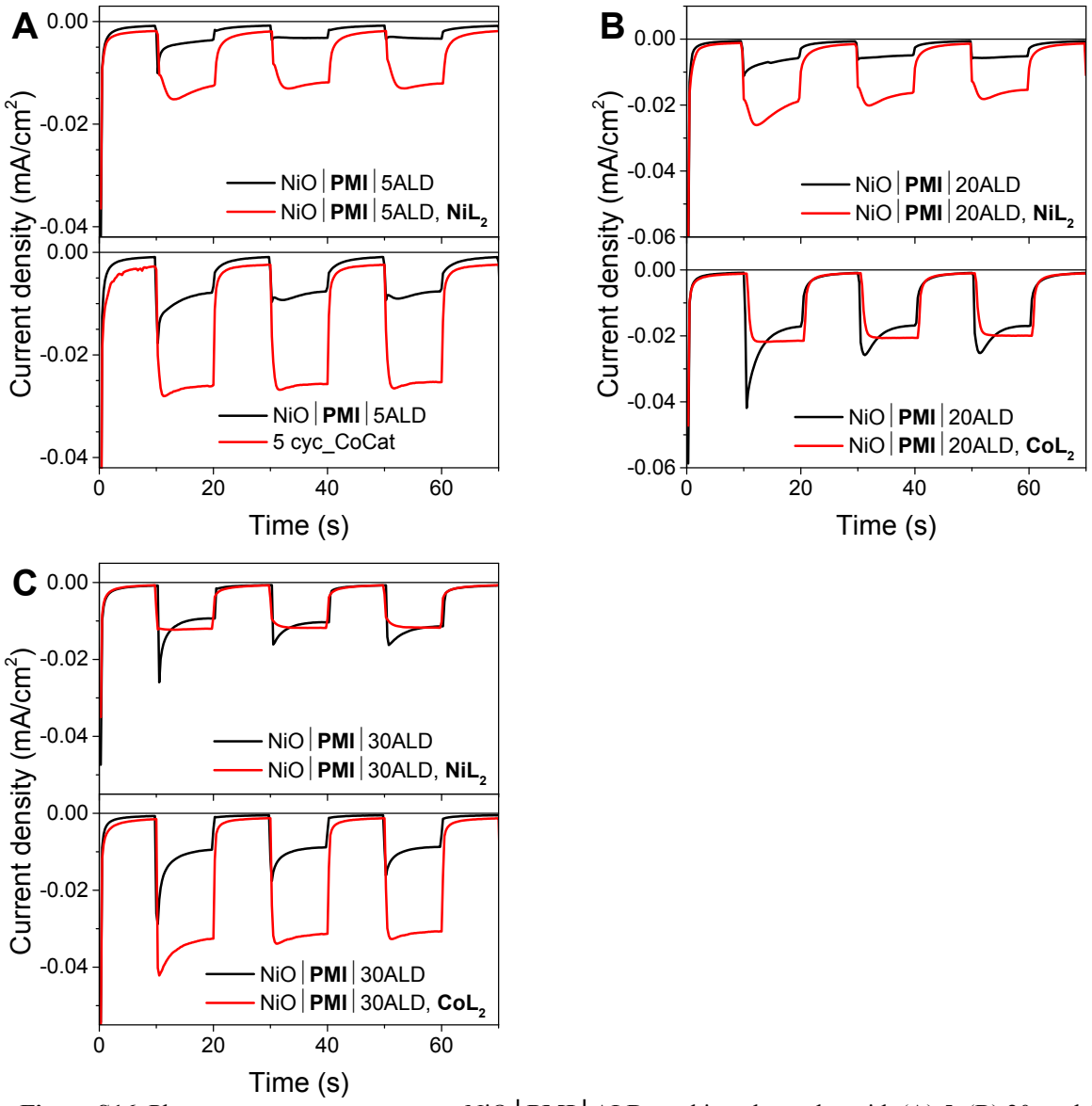

Figure S16. Photocurrent measurements on NiO | **PMI** | ALD working electrodes with (A) 5, (B) 20, and (C) 30 cycles of Al_2O_3 ALD with 10 s light on/off cycles and -0.40 V applied bias. Measurements were first made on NiO | **PMI** | ALD films (black) followed by addition of 0.5 mM **NiL$_2$** or 0.5 mM **CoL$_2$** (red). (Conditions: 0.1 M H_2SO_4 and 0.1 M Na_2SO_4 in 1:1 H_2O:MeCN; 200 mW/cm^2 white light with 410 nm long-pass filters; under argon; Ref = Ag/AgCl; Counter = GC; scan 5 mV/s from 0.00 V to -0.80 V)

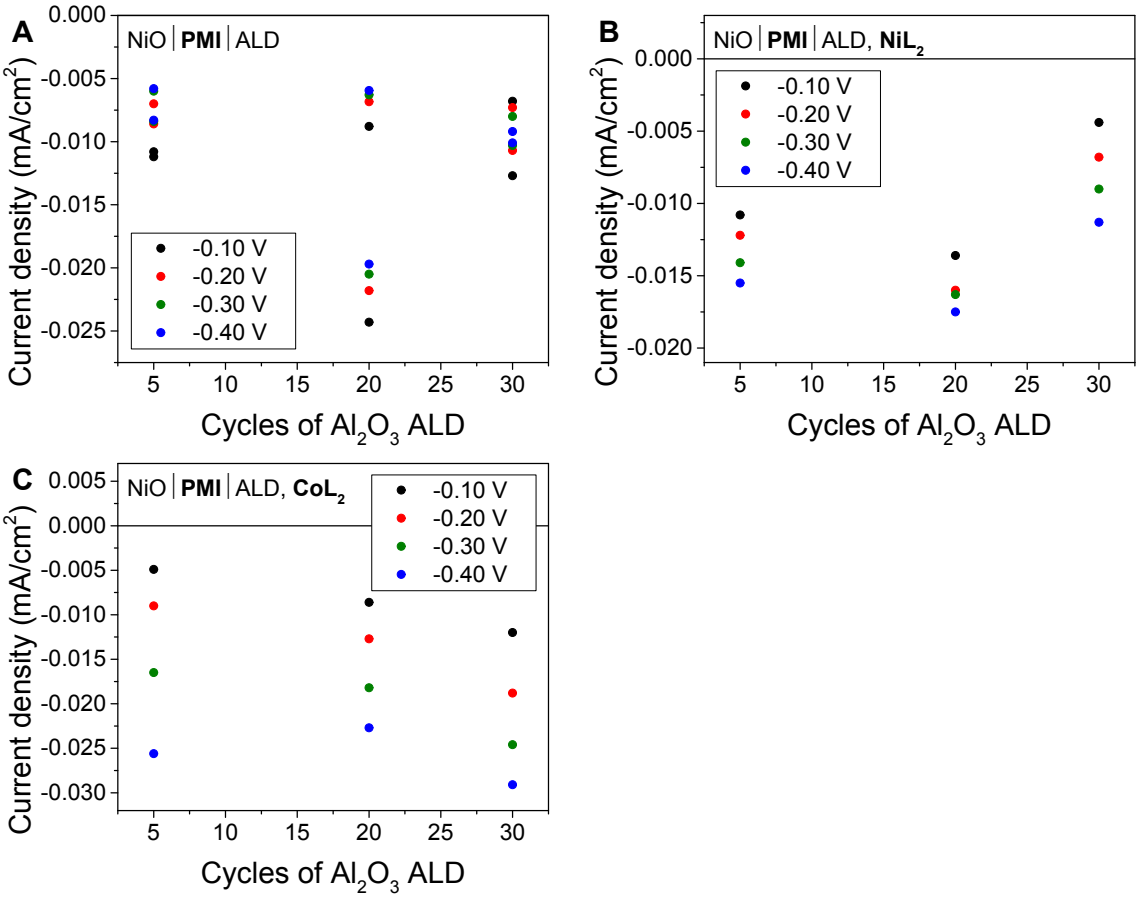

Figure S17. Current densities at the end of 10 s light cycles during the linear sweep voltammetry experiments reported in Figure S15 for NiO|**PMI**|ALD films with (A) 0-30 cycles of Al_2O_3 ALD and additional (B) 0.5 mM **NiL_2** or (C) 0.5 mM **CoL_2**. (Conditions: 0.1 M Na_2SO_4 and 0.1 M H_2SO_4 in 1:1 H_2O:MeCN; under argon; 200 mW/cm^2 white light with 410 nm long-pass filters; Ref = Ag/AgCl; Counter = GC)

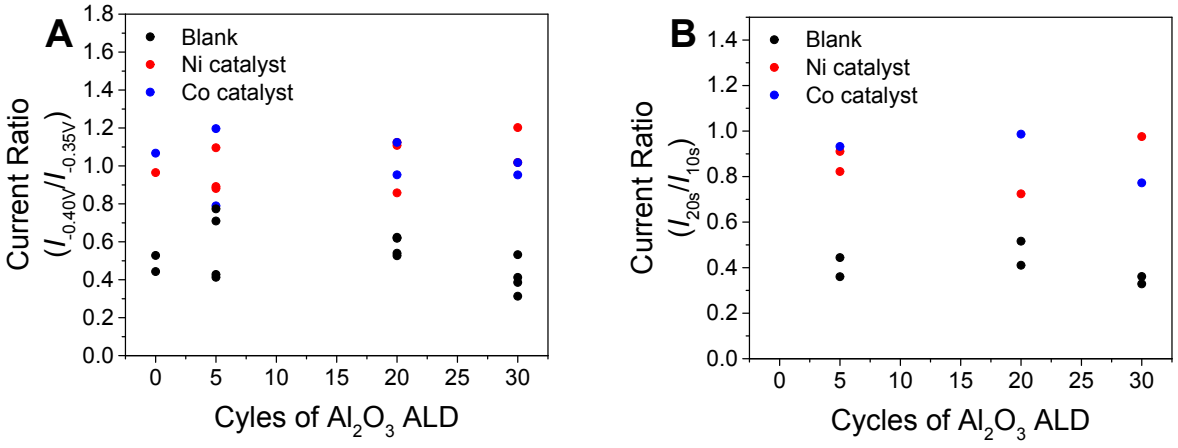

Figure S18. Ratios of current densities for photocurrent measurements for NiO|**PMI**|ALD films with 0-30 cycles of Al_2O_3 ALD (black) and then with additional 0.5 mM **NiL_2** (red) or 0.5 mM **CoL_2** (blue) from Figures S13, S15, and S16. (A) Ratio of current density at -0.40 V (light off) to that at -0.35 V (light on) for potential sweeps at 5 mV/s beginning at 0.00 V, in duplicate. (B) Ratio of current density at 20 s (light off) to that at 10 s (light on) during application of -0.40 V. (Conditions: 0.1 M Na_2SO_4 and 0.1 M H_2SO_4 in 1:1 H_2O:MeCN; under argon; 200 mW/cm^2 white light with 410 nm long-pass filters; Ref = Ag/AgCl; Counter = GC)

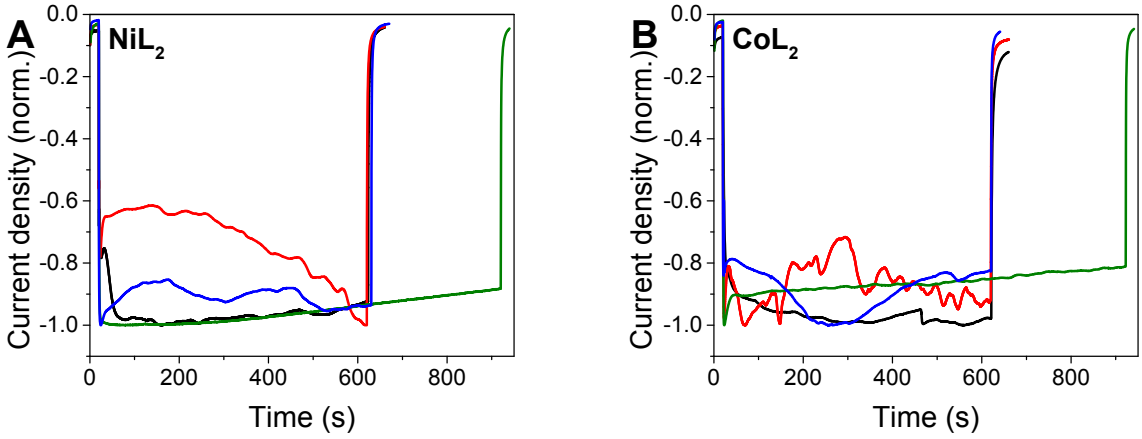

Figure S19. Normalized photocurrent density versus time for one light on-off cycle for NiO|**PMI**|ALD films with 0 (black), 5 (red), 20 (green), and 30 (blue) cycles of Al_2O_3 ALD and with (A) 0.5 mM **NiL_2** or (B) 0.5 mM **CoL_2**. Photocurrent is normalized to the largest amplitude in order to compare stability between different films. (Conditions: 0.1 M Na_2SO_4 and 0.1 M H_2SO_4 in 1:1 H_2O:MeCN; under argon; 200 mW/cm^2 white light with 410 nm long-pass filters; Ref = Ag/AgCl; Counter = GC; apply -0.40 V vs Ag/AgCl)

VI. Detection of evolved hydrogen

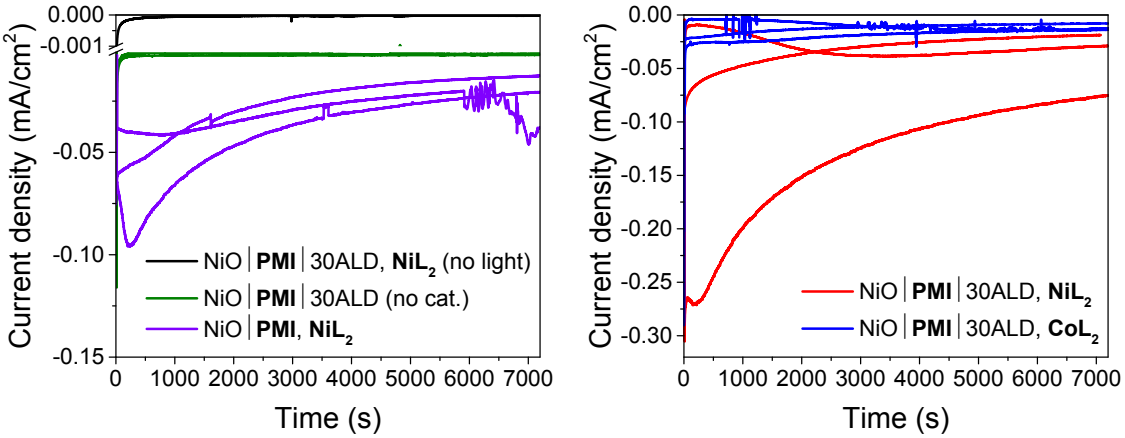

Figure S20. Photocurrent over two hours with -0.40 V vs Ag/AgCl applied bias for NiO|**PMI**|0 or 30ALD films with and without light and with and without 0.5 mM **NiL$_2$** or **CoL$_2$**. One to three separate films are shown for each set of conditions. (Conditions: 0.1 M Na_2SO_4 and 0.1 M H_2SO_4 in 1:1 H_2O:MeCN; under argon; 200 mW/cm^2 white light with 410 nm long-pass filters; Ref = Ag/AgCl; Counter = GC)

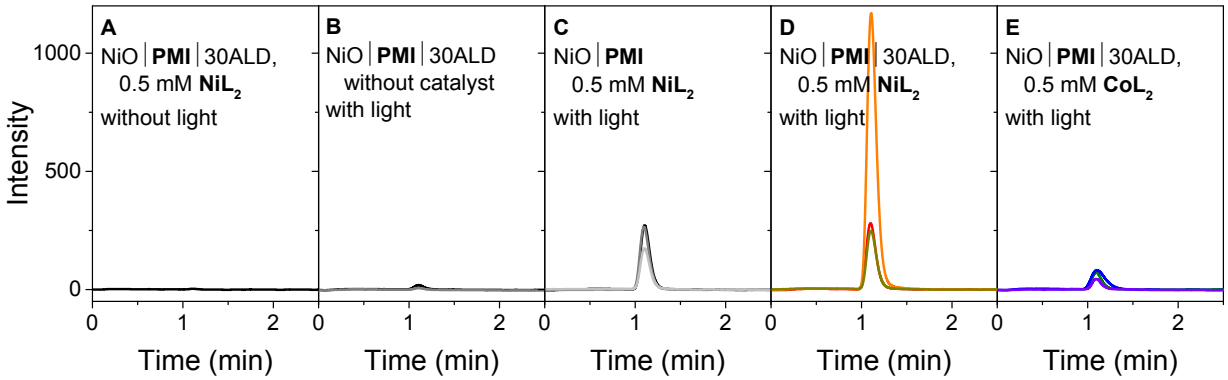

Figure S21. Hydrogen detected by gas chromatography after two hours with -0.40 V vs Ag/AgCl applied bias for NiO|**PMI**|30ALD films (A) 0.5 mM **NiL$_2$** without light, (B) without catalyst with light, (C) 0ALD with 0.5 mM **NiL$_2$** with light, (D) 0.5 mM **NiL$_2$** with light, and (E) 0.5 mM **CoL$_2$** with light, resulting from experiments in Figure S20. One to three separate films are shown for each set of conditions. Injections of 300 µL were made from the 20.2 mL headspace. (Conditions: 0.1 M Na_2SO_4 and 0.1 M H_2SO_4 in 1:1 H_2O:MeCN; under argon; 200 mW/cm^2 white light with 410 nm long-pass filters; Ref = Ag/AgCl; Counter = GC)

Table S2. Calculation of Faradaic efficiencies

	Volume H_2 in headspace (μL)	Charge passed (C)	Faradaic efficiency (%)
NiO | **PMI** | 30ALD, **NiL_2**, no light [a]	0.09	0.00015	-
NiO | **PMI** | 30ALD [b]	0.5 ± 0.3	0.007 ± 0.002	50 ± 30
NiO | **PMI**, **NiL_2** [b]	9 ± 2	0.09 ± 0.02	80 ± 10
NiO | **PMI** | 30ALD, **NiL_2** [b] (exclude high-performing outlier)	10.9 ± 0.3	0.086 ± 0.002	98 ± 4 [c]
NiO | **PMI** | 30ALD, **NiL_2** [a] (high-performing outlier)	45	0.37	94
NiO | **PMI** | 30ALD, **CoL_2** [b]	3 ± 2	0.04 ± 0.01	60 ± 10

[a] One sample studied.
[b] Average of two or three samples ± standard deviation.
[c]-Value includes the high-performing outlier.

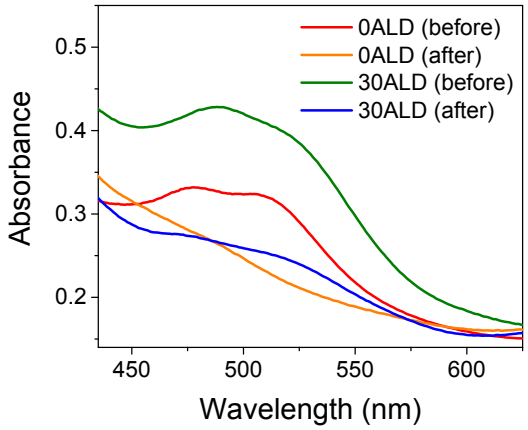

Figure S22. UV-vis absorption spectra of NiO | **PMI** films with 0 and 30 cycles of Al_2O_3 ALD before and after hydrogen evolution with **NiL_2** (Figures S20-S21). The NiO background is not subtracted.

VII. DFT-computed ground state structure

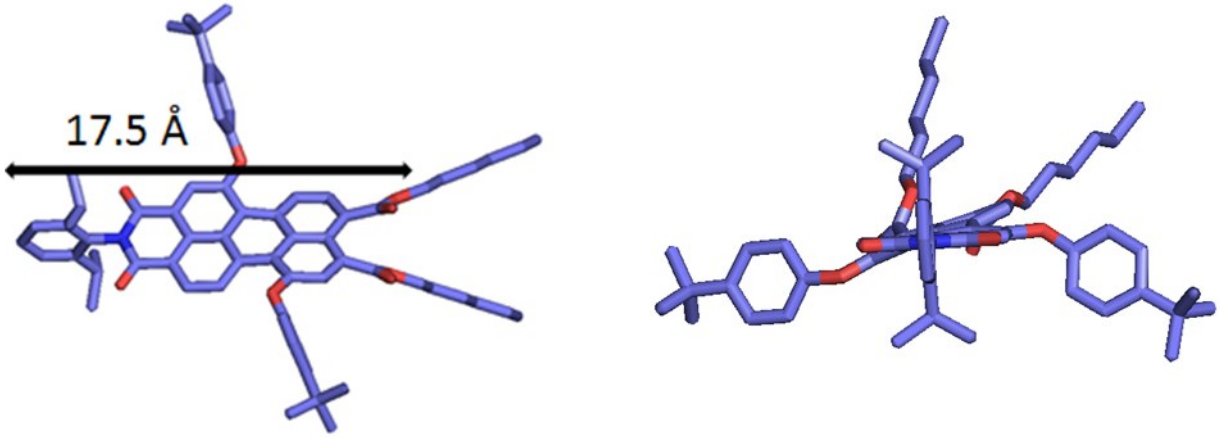

Figure S23. Optimized ground state geometry of **PMI diester** indicating the estimated height of the molecule from the NiO surface. Hydrogen atoms are omitted for clarity.

Table S3. Geometry of the electronic ground state (S_0) of **PMI diester** optimized with DFT (B3LYP/6-31G*). The absolute energy is -3293.107001 E_h.

C	-2.7633182414	3.7751171214	-0.4213947520
C	-2.8051717832	2.4271260793	-0.0565862053
C	-1.6428409933	1.6717047782	0.1518647097
C	-0.3787551628	2.3038058358	-0.0920347324
C	-0.3513495153	3.7021337407	-0.3899759828
C	-1.5521337509	4.4294054580	-0.5594131529
C	0.8431699729	1.5582522600	-0.0307571107
C	2.0482276951	2.2878565397	-0.0932956490
C	2.0651567321	3.6679717008	-0.3488794758
C	0.8905997876	4.3663668817	-0.5258307429
C	-1.6659706613	0.2663146429	0.5908402570
C	-0.4768785151	-0.5324061346	0.4542549708
C	0.7632160642	0.0938443213	0.0743927432
C	-2.8004522674	-0.3549491504	1.1387862052
C	-2.8401373167	-1.7414912521	1.3417661880
C	-1.7627403455	-2.5458878999	1.0415569674
C	-0.5104829801	-1.9576494595	0.6820442326
C	0.6996266123	-2.7116291820	0.5455533861
C	1.8294882968	-2.0949890161	0.0411954739
C	1.8597501674	-0.7200996200	-0.2031583380
C	0.9600497218	5.8093435165	-0.8612518210
N	-0.2673378565	6.4707144912	-1.0402951395
C	-1.5355777060	5.8678869978	-0.9058318836
O	-2.5553360173	6.5198081853	-1.0810087924
O	2.0205818942	6.4060497855	-0.9849611698
C	-0.2281074610	7.8723596896	-1.4186862659

C	-2.0982457770	-4.0085160747	1.0212734806
O	-2.8840993641	-4.5365430625	1.7773853623
C	0.8686248104	-4.0837213807	1.1126601037
O	0.3303072100	-4.4913240684	2.1233678937
O	-1.5466984018	-4.6339563518	-0.0442857539
O	1.7801533248	-4.8050590909	0.4200196858
C	-1.8536586958	-6.0418712760	-0.1605310733
C	-1.2187568550	-6.5552737041	-1.4436306085
C	-1.4838716489	-8.0518201969	-1.6551586725
C	-0.8532164530	-8.6038104232	-2.9400289496
C	-1.1135216760	-10.1005325318	-3.1518388727
C	2.1441919407	-6.0841978967	0.9856283550
C	3.1220483602	-6.7493624598	0.0295935358
C	3.5869014485	-8.1214677685	0.5366017248
C	4.5560441479	-8.8207906619	-0.4254899635
C	5.0288186182	-10.1921369215	0.0738407584
O	3.2533649490	1.6300454796	0.0290493686
O	-3.8747892169	0.4203624369	1.4948850448
C	-5.1544205978	-0.1146657413	1.6150290789
C	4.3156709316	2.2391119076	0.6889333796
C	-5.7845256102	-0.7569811850	0.5523079505
C	-7.0985262718	-1.2043140762	0.7040975652
C	-7.8122734374	-1.0111499739	1.8955095848
C	-7.1492456502	-0.3390472204	2.9369563289
C	-5.8351346509	0.1036785514	2.8105759780
C	5.5683504485	2.1820186215	0.0809914573
C	6.6754661867	2.6984188494	0.7485131576
C	6.5697242277	3.2868708670	2.0208926768
C	5.2936344460	3.3279754341	2.6002690108
C	4.1717399931	2.8073654960	1.9521161090
C	-0.2118228322	8.2012165992	-2.7856443912
C	-0.1791818507	9.5574636984	-3.1290172810
C	-0.1629678828	10.5463206539	-2.1498759672
C	-0.1793103514	10.1922409957	-0.8042197966
C	-0.2130523647	8.8495117486	-0.4097861220
C	-0.2344157425	8.4983094302	1.0728500851
C	1.0407782585	8.9874043696	1.7860543877
C	-1.5081502337	9.0300512684	1.7576035155
C	-0.2265703461	7.1423670820	-3.8814112298
C	-1.4910317326	7.2489693055	-4.7554564947
C	1.0580759668	7.1913012373	-4.7306104335
C	7.8265007799	3.8388190352	2.7174744791
C	8.8319771053	2.6835585931	2.9421086108
C	8.4821383808	4.9214865578	1.8276335627
C	7.5080078930	4.4725536861	4.0846147931
C	-9.2583844149	-1.4991985700	2.0949336336

C	-9.7949344463	-2.2541001971	0.8633763024
C	-9.3126735242	-2.4615682737	3.3058475779
C	-10.1796187013	-0.2853493863	2.3585467981
C	-0.4866358576	-10.6466323000	-4.4386205451
C	5.9937138825	-10.8852749138	-0.8935787442
H	-3.6807998065	4.3313730597	-0.5816114484
H	-3.7715268153	1.9677643545	0.0724193011
H	3.0091604382	4.1937658964	-0.4337089960
H	-3.7527258087	-2.2095366940	1.6890005334
H	2.7308585358	-2.6786388230	-0.1042222338
H	2.7753438025	-0.2829189897	-0.5668566101
H	-1.4666332186	-6.5543902627	0.7269348373
H	-2.9416519116	-6.1651417471	-0.1649020227
H	-1.6123121724	-5.9809038928	-2.2924015862
H	-0.1384259723	-6.3634446629	-1.4115272376
H	-1.1018507809	-8.6164542988	-0.7917891326
H	-2.5687596155	-8.2310749285	-1.6782058574
H	-1.2371494179	-8.0424063769	-3.8045253161
H	0.2321400808	-8.4241238621	-2.9202879928
H	-0.7256781870	-10.6601882425	-2.2887763622
H	-2.1978361441	-10.2803176132	-3.1674486622
H	2.5856597927	-5.9214785736	1.9754030238
H	1.2384665417	-6.6834238609	1.1249433538
H	2.6421025727	-6.8567709037	-0.9522951502
H	3.9880598338	-6.0904549592	-0.1154631077
H	4.0703954952	-8.0055926539	1.5175317842
H	2.7123626744	-8.7674156988	0.7018865109
H	4.0708312983	-8.9389631710	-1.4057194881
H	5.4297263382	-8.1745070029	-0.5947695973
H	5.5146405759	-10.0729017068	1.0526330514
H	4.1546376697	-10.8362011778	0.2445105994
H	-5.2536894374	-0.9132628947	-0.3820618631
H	-7.5636516686	-1.7081055363	-0.1355060952
H	-7.6629097999	-0.1619479815	3.8773120229
H	-5.3312629547	0.6172973248	3.6231596633
H	5.6628745388	1.7334725149	-0.9031013219
H	7.6429343082	2.6435688599	0.2582357840
H	5.1542915053	3.7661104203	3.5819648298
H	3.1966931116	2.8363105619	2.4281532563
H	-0.1656053348	9.8399163932	-4.1780379980
H	-0.1371727059	11.5947894257	-2.4354754814
H	-0.1667046655	10.9697875612	-0.0453806372
H	-0.2529076468	7.4077334983	1.1641407097
H	1.0306305915	8.6796081051	2.8387249643
H	1.9359417402	8.5714594062	1.3122706357
H	1.1212100163	10.0805343397	1.7606211432

H	-1.5309403137	8.7249750693	2.8107972217
H	-2.4063255174	8.6425937503	1.2657388370
H	-1.5518500515	10.1251530843	1.7274189635
H	-0.2540895565	6.1597267382	-3.4009822534
H	-1.5103029669	6.4402765091	-5.4958540113
H	-2.3951358849	7.1782552175	-4.1419490615
H	-1.5256552629	8.1998235230	-5.3004616890
H	1.0559859332	6.3822181215	-5.4708662742
H	1.9463711555	7.0806010212	-4.0998599580
H	1.1453137714	8.1396550701	-5.2740153084
H	9.7441853212	3.0581626686	3.4222862044
H	8.4011053336	1.9091801734	3.5868827191
H	9.1226954641	2.2096342079	1.9986669572
H	9.3882303146	5.3087296691	2.3089922367
H	7.7984218555	5.7615868018	1.6617552703
H	8.7704849142	4.5266764742	0.8478492064
H	7.0820951219	3.7441448862	4.7840254818
H	8.4292598279	4.8597362863	4.5338625525
H	6.8076147499	5.3103260113	3.9921893939
H	-10.8179220196	-2.5948148172	1.0580011665
H	-9.8255920943	-1.6169584314	-0.0278889411
H	-9.1902084723	-3.1388932283	0.6348869140
H	-10.3370648060	-2.8216953444	3.4602294859
H	-8.9890866006	-1.9745986086	4.2316260043
H	-8.6667908213	-3.3314306817	3.1424996240
H	-10.1695247045	0.4050555616	1.5075345422
H	-11.2128496748	-0.6177468819	2.5161525330
H	-9.8711495900	0.2760005755	3.2470056339
H	-0.6833952366	-11.7183314798	-4.5557633381
H	-0.8871445893	-10.1362761756	-5.3231977655
H	0.6013759047	-10.5059365195	-4.4410056997
H	6.3150256200	-11.8594367959	-0.5081539656
H	5.5238446554	-11.0515889039	-1.8707656324
H	6.8926067292	-10.2786492669	-1.0582232145

VIII. References

1. R. J. Lindquist, B. T. Phelan, A. Reynal, E. A. Margulies, L. E. Shoer, J. R. Durrant and M. R. Wasielewski, *J. Mater. Chem. A*, 2016, **4**, 2880-2893.
2. A. Bakac and J. H. Espenson, *J. Am. Chem. Soc.*, 1984, **106**, 5197-5202.
3. W. A. Hoffert, J. A. S. Roberts, R. M. Bullock and M. L. Helm, *Chem. Commun.*, 2013, **49**, 7767-7769.
4. S. Sumikura, S. Mori, S. Shimizu, H. Usami and E. Suzuki, *J. Photochem. Photobiol. A*, 2008, **199**, 1-7.

5. M. D. Hanwell, D. E. Curtis, D. C. Lonie, T. Vandermeersch, E. Zurek and G. R. Hutchison, *J. Cheminf.*, 2012, **4**, 17.
6. I. S. Ufimtsev and T. J. Martinez, *J. Chem. Theory Comput.*, 2009, **5**, 2619-2628.
7. A. D. Becke, *J. Chem. Phys.*, 1993, **98**, 5648-5652.
8. C. Lee, W. Yang and R. G. Parr, *Phys. Rev. B: Condens. Matter*, 1988, **37**, 785-789.
9. S. H. Vosko, L. Wilk and M. Nusair, *Can. J. Phys.*, 1980, **58**, 1200-1211.
10. P. J. Stephens, F. J. Devlin, C. F. Chabalowski and M. J. Frisch, *J. Phys. Chem.*, 1994, **98**, 11623-11627.
11. The PyMOL Molecular Graphics System (Version 1.7.4), Schrödinger, LLC, 2010.
12. R. M. Young, S. M. Dyar, J. C. Barnes, M. Juríček, J. F. Stoddart, D. T. Co and M. R. Wasielewski, *J. Phys. Chem. A*, 2013, **117**, 12438-12448.
13. MATLAB The MathWorks, Inc., Natick, Massachusetts, United States, 2010.